

## Experimental investigation of effect of printing direction and surface roughness on the mechanical properties of AlSi10Mg-alloy produced by selective laser melting

Dmitry Vysochinskiy, Naureen Akhtar, Tord Nordmo, Mathias Rabjerg Strand, Adrian Vyssios and Morten Kollerup Bak

Dmitry Vysochinskiy. University of Agder, Norway. Corresponding author: Dr. Dmitry Vysochinskiy, E-mail address:

dmitry.vysochinskiy@uia.no

Naureen Akhtar. University of Agder, Norway

Tord Nordmo. University of Agder, Norway

Mathias Rabjerg Strand. University of Agder, Norway

Adrian Vyssios. University of Agder, Norway

Morten Kollerup Bak. University of Agder, Norway

Mechatronics Innovation Lab AS, Norway

**Abstract.** The additive manufacturing has initially gained popularity for production of non-loadbearing parts and components or in the fields where the material strength and ductility are less important such as modelling and rapid prototyping. But as the technology develops, availability of metal additive manufacturing naturally dictates the desire to use the produced components in load-bearing parts. This requires not-only a thorough documentation on the mechanical properties but also additional and independent research to learn the expected level of variation of the mechanical properties and what factors affect them. The presented paper investigates strength, ductility, hardness, and microstructure of the AlSi10Mg alloy produced by the selective laser melting (SLM). The mechanical properties were determined through a series of uniaxial tension tests and supplementary hardness tests and rationalized with the microstructure evolution with regard to printing direction and heat treatment. The paper also addresses the effect of surface roughness on the mechanical properties of the material, by comparing the machined and net shape tension samples. As expected, the as-manufactured AlSi10Mg-alloy appears to be a semi-brittle alloy, but its microstructure can be altered, and ductility increased by a proper heat-treatment. The effect of surface layer removal on the measured mechanical properties is of particular interest.

**Keywords.** AlSi10Mg, Selective Laser Melting, Anisotropy, Surface Roughness, Additive Manufacturing, 3D Printing

## 1 Introduction

AlSi10Mg-alloy is originally a casting alloy which has become the most common aluminum alloy powder for metal additive manufacturing available at the market today. One common technology involved is selective laser melting (SLM), a type of powder bed fusion (PBF). The alloy undergoes much higher cooling rates under SLM process in comparison with casting which leads to a different microstructure. It is important to know how the properties are affected by the process, that is why the mechanical properties of additively manufactured AlSi10Mg, its microstructure and response to heat treatments have been actively studied by the research community in recent years. The researchers strive to understand the material microstructure, its properties and how are they affected by the process parameters. A paper on dynamic properties of AlSi10Mg by Maconachie et al. [1] presents a good overview of the static strength properties of AlSi10Mg reported in the literature; it is reported that SLM produced AlSi10Mg is expected to have yield strength about  $250 \pm 15$  MPa, tensile strength about  $360 \pm 57$  MPa and elongation at fracture about  $4.0 \pm 2.0$  % based on the literature review in [1]. Those values have increased slightly in recent publications and material certificates, supposedly due to improvement of powder composition and optimization of manufacturing parameters as the SLM-technology matures. The layer-wise SLM build-up makes material anisotropic. It displays higher strength and ductility in direction parallel to the melting layers and lower strength and ductility in direction normal to the layers, as the melt-pools and

layer boundaries consist of more brittle silicon-rich phases and act as brittle elements [2]. This anisotropic behavior in tension is observed in all reviewed studies that test different directions [1]–[7]. The ductility of the SLM manufactured AlSi10Mg-alloy is initially low but can be significantly increased by a heat treatment; an increase from about 5 up to more than 20 % elongation at fracture has been reported [8]; similar results were also observed by other researchers [9]–[12]. The increase in ductility comes at the cost of reduced strength, as usual. Fracture and fatigue behavior of SLM AlSi10Mg-alloy is also actively studied, but those properties are outside the scope of this article and the interested readers are referred to a recent review on fracture of additively manufactured components by Khosravani et al. [13].

Many authors, including [13], mention lack of standards for testing of mechanical properties of the additively manufactured components. Today's testing standards and approach to sample production reflect the traditional manufacturing techniques where a relatively large bulk of material is produced by casting, rolling or extrusion. The test samples are commonly manufactured out of the bulk of material by subtractive manufacturing techniques. In case of casting and hot rolling, where rough surface is produced, these surfaces are machined away to produce the smooth samples for mechanical testing. In case of thin-walled extrusions and cold-rolled metal sheets the initial surface is often deemed to be smooth enough and left untreated for sample production. Since AlSi10Mg-alloy is originally a casting alloy and additive manufacturing produces rough surfaces it is not surprising that most researchers adopt the sample production technique common for cast goods where a cylindrical sample is produced out of a bulk of material. This approach was used by above mentioned [1]–[5], while [6] used flat samples that were machined from all the sides and only [7] used flat sample cut out of thin-walled box with two surfaces left as-is i.e. rough. Examples of use of samples with all surfaces left unmachined were found in the literature not for aluminum, but for steel in case of uniaxial tension and high throughput characterization [14]. Both [7] and [14] tried to accommodate surface roughness by employing a corrected net cross-section area.

Using samples produced by subtractive manufacturing to determine the properties of materials produced by additive manufacturing is not a good match. The AM's flexibility naturally leads to minimization of material volume and production of thinner structures combined with rough surface. It is common to produce structures with large surface to volume ratio like in [10] and [15], thus effect of surface becomes significant and the use of machined samples need to be justified. While rough surface is commonly known to be one of the challenges connected to AM production [13].

In this article we make an attempt to quantify the effect of the surface on material behavior by making a direct comparison between machined and net shape samples of the same diameter and comparison of samples with different diameters. No such results were found in the reviewed literature. [16] performed a comparison of fatigue properties of machined and net shape samples but did not report effect of rough surface on behavior under uniaxial tension. The rest of the experimental work in the presented article is aimed at reproduction of the results reported in the literature. The article is based on the result reported in the master thesis performed at the University of Agder [17].

## 2 Materials and methods

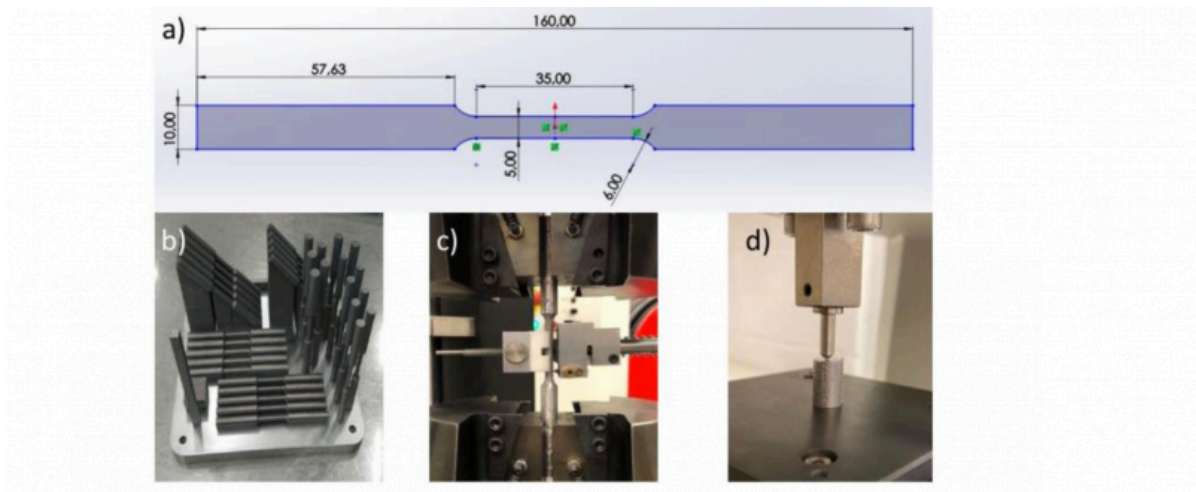


Fig. 1. Tensile sample geometry (a), samples on the build plate (b), tensile test with extensometer (c) and hardness test (d).

AlSi10Mg-alloy powder produced by plasma spheroidization and containing 9.25 %wt of Si and 0.26 %wt Mg was acquired from TEKNA advanced material [18]. The mechanical properties of the alloy were investigated through a series of uniaxial tension tests followed by supplementary hardness tests and microscopic investigation of the microstructure. 15 sample series, each consisting of 5 tension samples, were produced. The samples were cylindrical; the geometry of samples with 5 mm diameter is illustrated in Fig. 1a; samples with larger and smaller diameter were made as a scaled version of this sample keeping dimensions proportional. The net shape samples were printed with nominal dimensions while machined samples were printed with 1 mm surplus diameter and then machined using a lathe machine. Stress relief heat treatment was performed by heating the samples up to 300 °C in a furnace, soaking for 2 hours at this temperature and slowly cooling with the furnace turned off. An overview of the sample series is given in Table 1 in Results section. SLM@280 metal printer with 400 W laser was used to print the samples; argon gas was used as protective atmosphere and the printing layer thickness was set to 50  $\mu\text{m}$ . 25 kN SI-plan tension machine with hydraulic grips was used to perform tension tests. The machine is equipped with load cell, build-in position sensor and clip-on LVDT-based extensometer with measurement range 25 mm to 30 mm (Fig. 1c). The load-elongation curves were constructed using a combination of machine build-in sensors and extensometer displacement data and applying compliance correction where necessary. Supplementary Vickers hardness tests (HV5) were performed in accordance with ISO 6507 standard [19] using ZHU250CL Universal Hardness Tester. For microscopy and hardness testing, samples were cut from the end of uniaxial tension samples and the surface was polished. The test surface plane is thus perpendicular to the cylinder axis as shown in Fig. 1(d). The microstructures were investigated using Scanning Electron Microscope Jeol JSM-7200F.

## 3 Results

Table 1. Results overview,  $\pm$  indicate standard deviations.

Table 1 Results overview, ± indicate standard deviations

Series ID	Yield strength [MPa]	Tensile strength [MPa]	Elongation at fracture [%]	Hardness HV5	Orientation	Nominal Diameter [mm]	Machined / Net shape	Heat treatment
1	234.8±3.4	379.8±5.2	6.6±0.5	131.4±0.9	Horizontal	5.0	Net shape	As-built
2	229.8±3.6	394.2±6.7	6.05±0.3	119.2±3.0	Inclined 45°	5.0	Net shape	As-built
3	229.8±2.8	408.5±9.7	6.61±0.7	118.9±4.1	Vertical	5.0	Net shape	As-built
4	260.8±2.1	431.9±3.0	12.60±0.5	-	Horizontal	5.0	Machined	As-built
5	228.3±2.3	425.0±6.9	9.22±0.5	-	Inclined 45°	5.0	Machined	As-built
6	219.0±4.4	402.2±8.6	5.68±0.5	-	Vertical	5.0	Machined	As-built
7	117.8±5.3	222.4±9.7	25.1±3.9	72.6±3.6	Horizontal	5.0	Machined	Stress relief
8	107.6±1.7	221.4±1.9	27.3±3.0	69.4±2.3	Inclined 45°	5.0	Machined	Stress relief
9	121.2±7.7	238.9±5.0	18.7±1.4	75.5±1.8	Vertical	5.0	Machined	Stress relief
10	223.0±4.5	402.7±8.2	-	-	Horizontal	2.5	Net shape	As-built
11	209.8±1.3	381.6±7.6	-	-	Vertical	2.5	Net shape	As-built
12	227.4±2.7	361.7±27.5	-	-	Horizontal	4.0	Net shape	As-built
13	212.8±2.8	414.8±8.6	-	-	Vertical	4.0	Net shape	As-built
14	235.3±1.3	396.0±3.4	-	-	Horizontal	6.0	Net shape	As-built
15	221.2±9.9	397.3±12.9	-	-	Vertical	6.0	Net shape	As-built

Table 1 gives an overview of the uniaxial tension tests results along with supplementary hardness tests when those were performed. Elongation at fracture is reported for the gauge length to diameter ratio equals 5 i.e. for the  $l_0 = 5d_0 = 5.65\sqrt{A_0}$ , which is the standard ratio for determination of ductility in most European standards including Eurocode 3 [20]. No ductility values are reported for the sample series 10-15 where the gauge length to diameter would be non-standard, hence no extensometer was used in those series.

Fig. 2 demonstrates engineering stress-strain curves from test series 1-3 and 4-6 making a comparison between the behavior of net shaped and machined samples. These samples demonstrate semi-brittle behavior and fail after some yield deformation but before formation of a neck. While machined samples display slightly higher strength and significantly higher ductility in direction normal to the build, the ductility of net shape samples appears to be nearly the same for all three orientations. This can be explained by the additional surface roughness introduced by the support structure, which is needed in case of production of inclined and horizontally oriented samples. The horizontally oriented samples obtain a rougher surface than the vertically oriented ones, as Fig. 2 indicates. Thus, the effect of higher ductility is cancelled out by higher surface roughness.

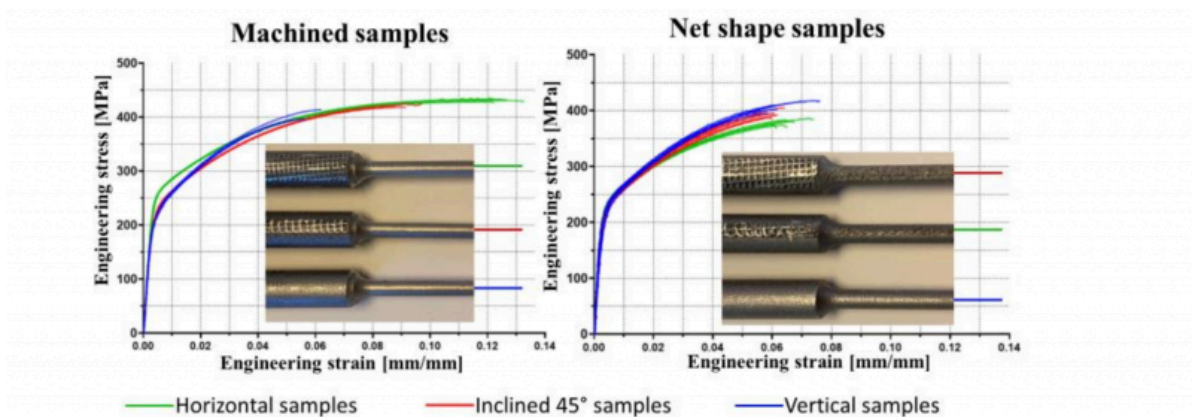


Fig. 2. Comparison of engineering stress strain curves for machined and net shape samples with different orientation.

Fig. 3 displays the SEM images of the microstructure of the as-built (left panel) and heat-treated samples (right panel)

oriented vertically i.e. with axis oriented in the build direction. The fibrous Si network around the Al matrix grains is evident in the as-built sample. Heat treatment led to the diffusion of the segregated Si and formation of particles [21]. Fig. 4 illustrates increase in ductility in all three direction by comparing 4-6 and 7-9 tensile test series. The heat-treated samples show ductile behavior and form a neck prior to fracture.

SEM study was also carried out for the fracture surfaces to understand the mechanism linked to the fracture of the samples. Figure 5 displays the fracture surfaces of the vertically oriented as-built (Fig. 5a-c) and heat-treated samples (Fig. 5d-f). Heat treated sample showed lower density of voids compared to as-built (Fig. 5a and 5d). High magnification SEM images for as-built samples showed two main morphologies in the form of stepped cleavage planes and dimples as shown in Fig. 5b and 5c respectively. The presence of ‘river pattern-like’ stepped cleavage planes shows a typical brittle fracture while presence of the dimple features is indicative of the ductile failure [8][22]. Heat treatment led to the disappearance of stepped cleavage planes (Fig. 5e). Moreover, dimple features are deeper in the heat-treated sample compared to the as-built indicating higher levels of plastic deformation prior to fracture. This is consistent with the higher ductility in the heat-treated samples.

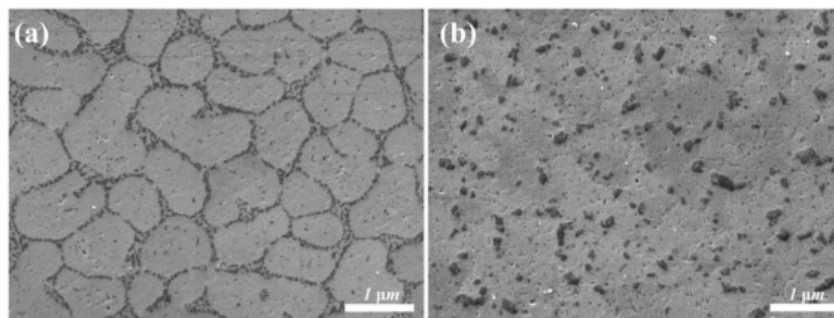


Fig. 3. SEM images for the as-built (a) and heat-treated (b) vertically oriented SLM AlSi10Mg samples.

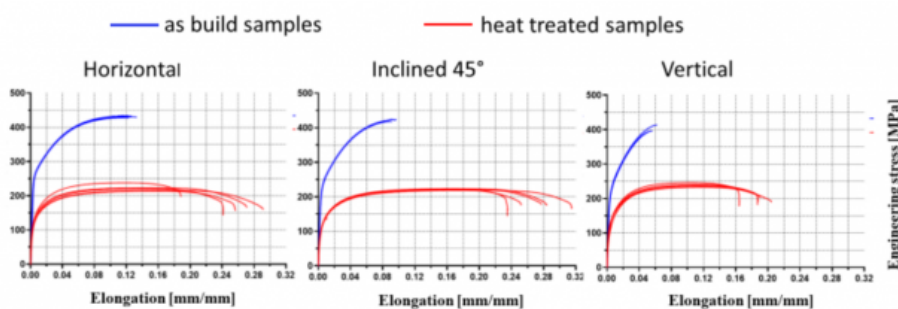


Fig. 4. Comparison of engineering stress strain curves for machined and net shape samples with different orientation.

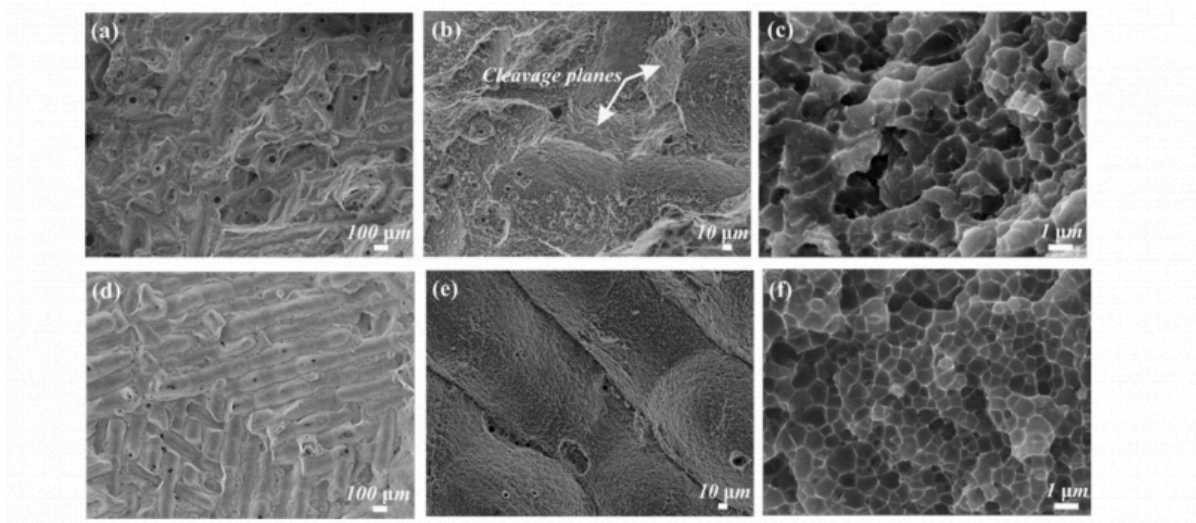


Fig. 5. SEM images of the fracture surfaces of the as-built sample (a-c) and heat-treated (d-f) sample with vertical orientation.

## 4 Discussions and Conclusions

The mechanical properties of SLM manufactured AlSi10Mg alloy are significantly affected by the powder quality and processing and printer settings, which complicates the direct quantitative comparison of the results with the ones reported in the literature; nevertheless, we can conclude that a good agreement on qualitative level is observed:

- Tested AlSi10Mg alloy displays anisotropy with samples oriented normal to the build directions displaying higher strength and ductility; same is observed in the literature [1]–[7]
- The directional variation in ductility is much greater, than variation in strength, when machined samples are viewed. The same is also observed in the literature. In fact, some authors report that variation in strength can be ignored, while acknowledging variation in ductility [1].
- The microstructure of the as-built AlSi10Mg alloy is similar to the one reported in the literature [1], [4], [5], [8], [11], [12]
- The heat treatment reduces the strength and increases the ductility of tested SLM produced AlSi10Mg alloy. The same is reported in the literature [5], [8], [10], [11], [21], although different authors used different heat treatments and effect varies depending on the treatment.

The quantitative comparison is more difficult. For example, for the studied AlSi10Mg alloy vertically oriented samples displayed 5.68 % elongation at fracture and horizontally oriented samples displayed 12.6 % elongation at fracture. The similar levels of ductility i.e. about 6 % for the build direction and 12 % for the horizontal direction were observed by [3]. [6] also reported the vertically oriented samples to have about half of the ductility of the horizontally oriented, but the level of ductility was half of the reported here, i.e. about 3 % and 6 % for vertically and horizontally oriented samples respectively. Other authors report both lower levels of ductility and less difference in ductility between directions [1], [2], [4].

However, the increased ductility in direction normal to the build i.e. parallel to the layers, is only observed in case when the original rough surface is removed. The need for support structure in case of horizontally oriented and inclined samples introduces additional surface roughness in the net shape samples. The rough surface promotes failure, and

the effect of higher ductility is canceled out by the rougher surface. The result is that the net shape tensile samples display about the same levels of ductility regardless of the direction. Curiously, the vertically oriented net shape samples display slightly higher ductility than the machined vertically oriented samples, thus no reduction of ductility due to rough surface was observed here. It can thus be speculated that the brittle borders between the build lays are so efficient in promoting fracture in those samples that the surface roughness difference between machined and net shape samples has no effect on measured ductility.

The effect of surface roughness on strength is even more interesting. Using the same approach as in [14], we can calculate the difference between actual cross-section area and measured one as:

$$\Delta A = A_{\text{measured}} - A_{\text{true}} = \frac{\pi}{4} (\bar{d}^2 - (\bar{d} - 2\bar{R}_p)^2) = \frac{\pi}{4} (4\bar{d}\bar{R}_p - 4\bar{R}_p^2) \quad (1)$$

where  $\bar{d}$  is the mean measured diameter and  $\bar{R}_p$  is the average peak roughness. If we assume that the average peak roughness does not depend on the printed cross-section size and the actual yield strength is constant, the detected yield strength should approach the actual yield strength asymptotically as the cross-section diameter increases:

$$\sigma_{0.2 \text{ measured}} = \frac{F}{A_{\text{measured}}} = \sigma_{0.2 \text{ true}} \frac{(\bar{d} - 2\bar{R}_p)^2}{\bar{d}^2} \quad (2)$$

According to Equation 2, the measured yield strength  $\sigma_{0.2 \text{ measured}}$  of the net shapes samples should increase as the diameter of the samples increases; this is indeed the case both for vertically and horizontally oriented samples as Table 1 indicates. On the other hand, machining of the samples reduces the surface roughness, and the measured strength should increase for machined samples in comparison with the net shape ones. This is not the case, machined vertically oriented samples display lower average yield strength than the net shape ones. This indicates that the removal of the surface layer by machining might have some additional effects on strength apart from reducing the surface roughness.

## Bibliography

- [1] T. Maconachie et al., "Effect of build orientation on the quasi-static and dynamic response of SLM AlSi10Mg," *Mater. Sci. Eng. A*, vol. 788, Jun. 2020, doi: 10.1016/j.msea.2020.139445.
- [2] I. Rosenthal, A. Stern, and N. Frage, "Strain rate sensitivity and fracture mechanism of AlSi10Mg parts produced by Selective Laser Melting," *Mater. Sci. Eng. A*, vol. 682, pp. 509–517, Jan. 2017, doi: 10.1016/j.msea.2016.11.070.
- [3] M. Kristoffersen, M. Costas, T. Koenis, V. Brøtan, C. O. Paulsen, and T. Børvik, "On the ballistic perforation resistance of additive manufactured AlSi10Mg aluminium plates," *Int. J. Impact Eng.*, vol. 137, p. 103476, Mar. 2020, doi: 10.1016/j.ijimpeng.2019.103476.
- [4] N. O. Larrosa et al., "Linking microstructure and processing defects to mechanical properties of selectively laser melted AlSi10Mg alloy," *Theor. Appl. Fract. Mech.*, vol. 98, no. September, pp. 123–133, Dec. 2018, doi: 10.1016/j.tafmec.2018.09.011.
- [5] A. Kempf and K. Hilgenberg, "Influence of sub-cell structure on the mechanical properties of AlSi10Mg manufactured by laser powder bed fusion," 2020, doi: 10.1016/j.msea.2020.138976.

- [6] L. Hitzler et al., "Direction and location dependency of selective laser melted AlSi10Mg specimens," *J. Mater. Process. Technol.*, vol. 243, pp. 48–61, May 2017, doi: 10.1016/j.jmatprotec.2016.11.029.
- [7] M. Costas, D. Morin, M. de Lucio, and M. Langseth, "Testing and simulation of additively manufactured AlSi10Mg components under quasi-static loading," *Eur. J. Mech. A/Solids*, vol. 81, p. 103966, May 2020, doi: 10.1016/j.euromechsol.2020.103966.
- [8] W. Li et al., "Effect of heat treatment on AlSi10Mg alloy fabricated by selective laser melting: Microstructure evolution, mechanical properties and fracture mechanism," *Mater. Sci. Eng. A*, vol. 663, pp. 116–125, Apr. 2016, doi: 10.1016/j.msea.2016.03.088.
- [9] L. Zhou, A. Mehta, E. Schulz, B. McWilliams, K. Cho, and Y. Sohn, "Microstructure, precipitates and hardness of selectively laser melted AlSi10Mg alloy before and after heat treatment," *Mater. Charact.*, 2018, doi: 10.1016/j.matchar.2018.04.022.
- [10] I. Maskery et al., "A mechanical property evaluation of graded density Al-Si10-Mg lattice structures manufactured by selective laser melting," 2016, doi: 10.1016/j.msea.2016.06.013.
- [11] M. Fousová, D. Dvorský, A. Michalcová, and D. Vojtěch, "Changes in the microstructure and mechanical properties of additively manufactured AlSi10Mg alloy after exposure to elevated temperatures," *Mater. Charact.*, vol. 137, pp. 119–126, Mar. 2018, doi: 10.1016/j.matchar.2018.01.028.
- [12] L. Girelli, M. Tocci, M. Gelfi, and A. Pola, "Study of heat treatment parameters for additively manufactured AlSi10Mg in comparison with corresponding cast alloy," *Mater. Sci. Eng. A*, vol. 739, pp. 317–328, Jan. 2019, doi: 10.1016/j.msea.2018.10.026.
- [13] M. R. Khosravani, F. Berto, M. R. Ayatollahi, and T. Reinicke, "Fracture behavior of additively manufactured components: A review," *Theor. Appl. Fract. Mech.*, vol. 109, no. July, p. 102763, 2020, doi: 10.1016/j.tafmec.2020.102763.
- [14] B. C. Salzbrenner et al., "High-throughput stochastic tensile performance of additively manufactured stainless steel," *J. Mater. Process. Technol.*, vol. 241, pp. 1–12, Mar. 2017, doi: 10.1016/j.jmatprotec.2016.10.023.
- [15] C. Bonatti and D. Mohr, "Mechanical performance of additively-manufactured anisotropic and isotropic smooth shell-lattice materials: Simulations & experiments," *J. Mech. Phys. Solids*, 2019, doi: 10.1016/j.jmps.2018.08.022.
- [16] A. D. Brandão, J. Gumpinger, M. Gschweidl, C. Seyfert, P. Hofbauer, and T. Ghidini, "Fatigue Properties of Additively Manufactured AlSi10Mg-Surface Treatment Effect," in *Procedia Structural Integrity*, 2017, vol. 7, pp. 58–66, doi: 10.1016/j.prostr.2017.11.061.
- [17] T. Nordmo, M. R. Strand, and A. Vyssios, "Mekaniske egenskaper til selektiv lasersmeltet AlSi10Mg-legering," University of Agder, 2020. Accessed: Nov. 24, 2020. [Online]. Available: <https://uia.brage.unit.no/uia-xmlui/handle/11250/2679275>.
- [18] "AlSiMg Aluminum Alloy Spherical Powder | Tekna." [http://www.tekna.com/spherical-powders/alsimg\\_aluminum\\_alloy](http://www.tekna.com/spherical-powders/alsimg_aluminum_alloy) (accessed Nov. 27, 2020).
- [19] International Organization for Standardization, "ISO 6507-1:2005 Metallic materials: vickers hardness test, part 1: Test method," Standard Norge Pronorm, Lysaker, 2006. [20] "EN 1993-1-1: Eurocode 3: Design of steel structures - Part 1-1: General rules and rules for buildings."
- [21] N. T. Aboulkhair, I. Maskery, C. Tuck, I. Ashcroft, and N. M. Everitt, "The microstructure and mechanical properties

of selectively laser melted AlSi10Mg: The effect of a conventional T6-like heat treatment," *Mater. Sci. Eng. A*, vol. 667, pp. 139–146, Jun. 2016, doi: 10.1016/j.msea.2016.04.092.

[22] J. Chen, W. Hou, X. Wang, S. Chu, and Z. Yang, "Microstructure, porosity and mechanical properties of selective laser melted AlSi10Mg," *Chinese J. Aeronaut.*, vol. 33, no. 7, pp. 2043–2054, Jul. 2020, doi: 10.1016/j.cja.2019.08.017.

PDF automatically generated on 2021-05-20 06:36:37

Article url: <https://popups.uliege.be/esaform21/index.php?id=3627>

published by ULiège Library in Open Access under the terms and conditions of the CC-BY License

(<https://creativecommons.org/licenses/by/4.0>)